



CDF note 8942

Direct Measurement of W Boson Charge Asymmetry with 1 fb^{-1} of Run II Data

The CDF Collaboration
URL <http://www-cdf.fnal.gov>
(Dated: October 10, 2008)

We present a new analysis method which directly reconstructs the W rapidity from $W \rightarrow e\nu$ data to measure the W boson charge asymmetry in $p\bar{p}$ collisions at $\sqrt{s} = 1.96 \text{ TeV}$ using an integrated luminosity of 1 fb^{-1} . The asymmetry provides new input on the momentum fraction dependence of the u and d quark parton distribution functions (PDF) within the proton.

I. INTRODUCTION

$W^+(W^-)$ bosons are produced in $p\bar{p}$ collisions primarily by the annihilation of $u(d)$ quarks from the proton and $\bar{d}(\bar{u})$ quarks from the anti-proton. As the u quark tends to carry a higher fraction of the proton's momentum than the d quark, the $W^+(W^-)$ is boosted, on average, in the proton (anti-proton) direction as shown in Figure 1.

The W^\pm charge asymmetry is defined as

$$A(y_W) = \frac{d\sigma(W^+)/dy_W - d\sigma(W^-)/dy_W}{d\sigma(W^+)/dy_W + d\sigma(W^-)/dy_W}, \quad (1)$$

where the subscript(+,-) denotes the charge of the W and y_W is the rapidity of the W bosons [1]. For $p\bar{p}$ collisions in leading-order parton model, $A(y_W)$ is given approximately by

$$A(y_W) \approx \frac{u(x_1)d(x_2) - d(x_1)u(x_2)}{u(x_1)d(x_2) + d(x_1)u(x_2)}, \quad (2)$$

where $x_{1,2} = x_0 e^{\pm y_W}$ and $x_0 = M_W/\sqrt{s}$. A precise measurement of the W asymmetry is a sensitive probe of the momentum fraction difference between u and d quarks in the $Q^2 \approx M_W^2$ region and is one of the best determinations of the proton d/u momentum ratio as a function of x , and plays an important role in global fits.

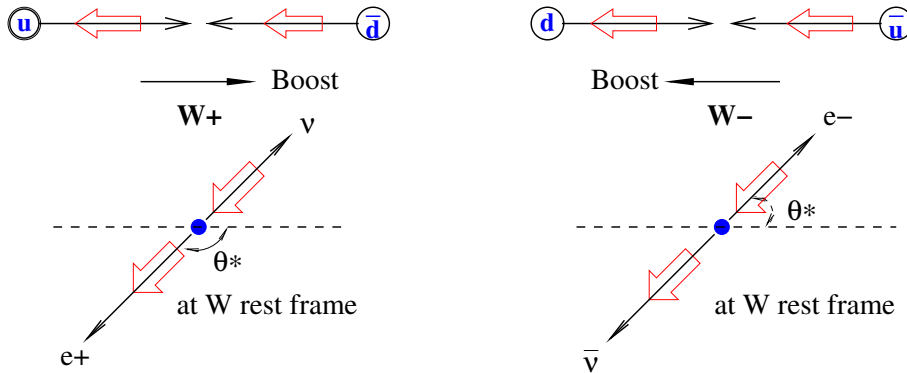


FIG. 1: The momenta (arrows) and helicities (large outlines of arrows) in $p\bar{p} \rightarrow W^\pm$ production and W^\pm leptonic decay in leading order.

The W decay, in our case $W^\pm \rightarrow e^\pm \nu$, provides a high purity sample for measuring this asymmetry. But since the p_z of the neutrino is unmeasured, the asymmetry has been measured traditionally [2] [3] as

$$A(\eta_e) = \frac{d\sigma(e^+)/d\eta_e - d\sigma(e^-)/d\eta_e}{d\sigma(e^+)/d\eta_e + d\sigma(e^-)/d\eta_e}, \quad (3)$$

where η_e is the electron pseudo-rapidity. By assuming that the $W \rightarrow e\nu$ decays are described by the Standard Model $V-A$ (vector-axial vector) couplings, the electron asymmetry, $A(\eta_e)$, is a convolution of W^\pm production and decay asymmetries, which results in a change in sign of $A(\eta_e)$ at high $|\eta_e|$. The predicted $A(y_W)$ and $A(\eta_e)$ are shown in Figure 2. However, we can determine the neutrino momentum up to a two-fold ambiguity by constraining the W mass. This ambiguity can be partly resolved on a statistical basis from the known $V-A$ decay distribution for the center-of-mass decay angle θ^* and of the W^\pm production cross-sections as a function of y_W , $d\sigma/dy$.

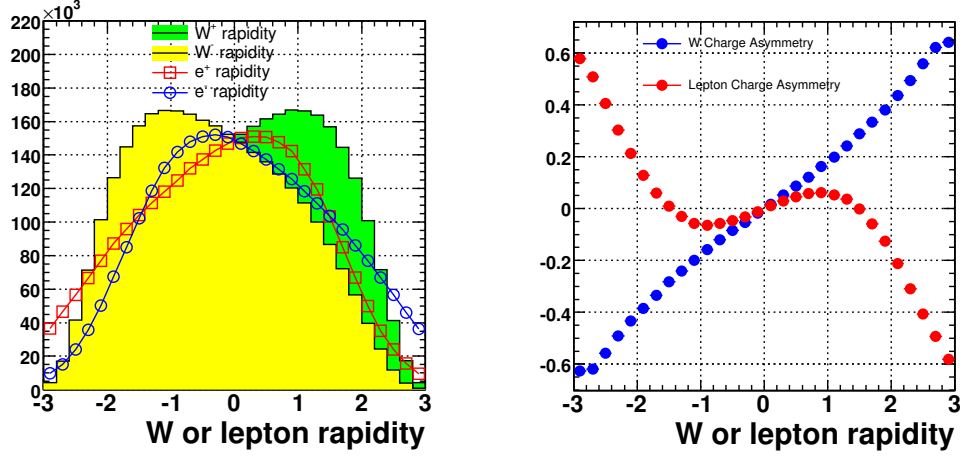


FIG. 2: The W boson and lepton rapidity distributions in $p\bar{p}$ collisions (left) and the relationship between the W production charge asymmetry and lepton charge asymmetry from the W leptonic decay as a function of rapidity (right).

We use the Monte Carlo to estimate the production probability of the two factors. First, in Figure 3 we verify the expected angular distribution of $(1 \pm \cos\theta)^2$ from the production of W^\pm with quarks in the proton and the opposite distribution with anti-quarks in the proton. The ratio of quark (proton) induced to anti-quark (proton) induced W production therefore determines the angular decay distribution. In the simulation, we measure the fraction of each, and parameterize the angular distributions as a function of y_W and the W transverse momentum, P_T^W . We find the functional form:

$$P_\pm(\cos\theta^*, y_W, p_T^W) = (1 \mp \cos\theta^*)^2 + Q(y_W, p_T^W)(1 \pm \cos\theta^*)^2, \quad (4)$$

$$Q(y_W, p_T^W) = f(p_T^W) e^{-[g(p_T^W) * y_W^2 + 0.05 * |y_W^3|]}, \quad (5)$$

where the functions $f(p_T^W)$ and $g(p_T^W)$ are

$$\begin{aligned} f(p_T^W) &= 0.2811\mathcal{L}(p_T^W, \mu = 21.7\text{GeV}, \sigma = 9.458\text{GeV}) \\ &\quad + 0.2185e^{(-0.04433\text{GeV}^{-1}p_T^W)}, \\ g(p_T^W) &= 0.2085 + 0.0074\text{GeV}^{-1}p_T^W \\ &\quad - 5.051 \times 10^{-5}\text{GeV}^{-2}p_T^W{}^2 \\ &\quad + 1.180 \times 10^{-7}\text{GeV}^{-3}p_T^W{}^3. \end{aligned} \quad (6)$$

where $\mathcal{L}(x, \mu, \sigma)$ is the Landau distribution with most probable value μ and the RMS σ . The first term of Eqn. 4 corresponds to contributions from quarks in the proton and the second term from anti-quarks in the proton. The parameterization in Eqn. 5, $Q(y_W, P_T^W)$ is obtained using MC@NLO including NLO QCD prediction [4].

The second relevant factor is the sum of the W^+ and W^- cross-sections as a function of y_W . As shown in Figure 2, W boson production decreases sharply beyond $|y_W| > 2$ because of the scarcity of high x quarks. Therefore, if two solutions are possible, one in the central region and another with $|y_W| > 2$, the former should receive more weight as the latter is very unlikely to be produced.

Finally, the weighting factor for each rapidity solution is represented as

$$wt_{1,2}^\pm = \frac{P_\pm(\cos\theta_{1,2}^*, y_{1,2}, P_T^W)\sigma_\pm(y_{1,2})}{P_\pm(\cos\theta_1^*, y_1, P_T^W)\sigma_\pm(y_1) + P_\pm(\cos\theta_2^*, y_2, P_T^W)\sigma_\pm(y_2)}, \quad (7)$$

where the \pm signs indicate the W boson charge and indices of 1, 2 are for the two W rapidity solutions. In Eqn 7, the weighting factor depends primarily on the W^+ and W^- cross-sections, but does have some weak dependence on the W charge asymmetry itself. Therefore, this method requires us to iterate the procedure to eliminate the dependence of the asymmetry on the weighting factor for our measurement.

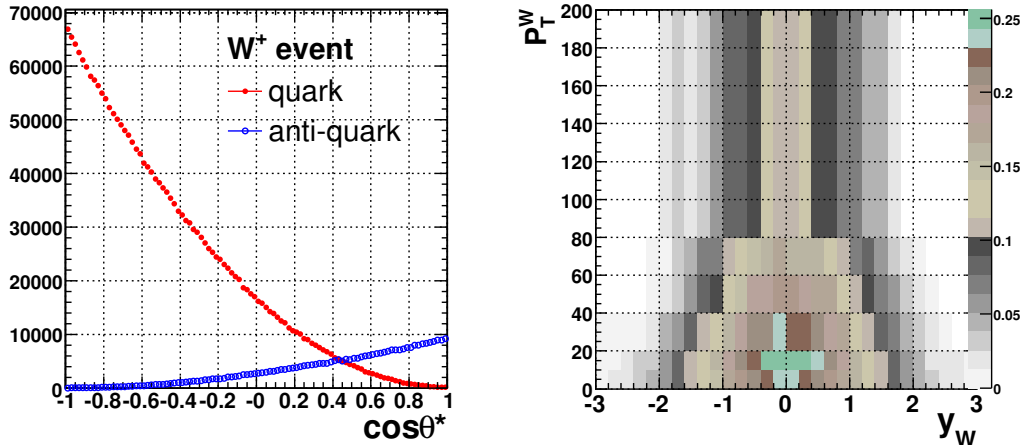


FIG. 3: The left plot shows the $\cos\theta^*$ distributions of e^+ in the W^+ rest frame, averaged over all produced W . The labeled “quark” curve shows the case where a quark from the proton and an anti-quark from the anti-proton form the W , and “anti-quark” is the opposite case (i.e. an anti-quark from the proton and a quark from the anti-proton). The right plot shows the dependence of the ratio of “anti-quark” (\bar{q}) and “quark” (q) contributions to the overall W decay angle distribution as a function of W rapidity and p_T of the W .

II. DATASET AND EVENT SELECTION

A. Dataset

We use high- p_T electron datasets in the central ($|\eta_e| < 1$) and plug regions ($1 < |\eta_e| < 2.8$), with an integrated luminosity of 1 fb^{-1} . All data runs used are required to pass our “good run” criteria for electrons with a working silicon detector. The following Monte Carlo samples are used to study the efficiencies of trigger and electron identification, the sensitivity of this new method and the systematics on the measurement of the W charge asymmetry. All Monte Carlo samples are generated with Pythia 6.216 (CTEQ5L), passed through the full simulation of the CDF detector and reconstructed.

- 19.8 million $W \rightarrow e\nu$ events
- 16.3 million $W \rightarrow \tau\nu$ events
- 10.1 million $Z \rightarrow e^+e^-$ events
- 9.7 million $Z \rightarrow \tau^+\tau^-$ events

B. Event Selection

The criteria used to identify the electron and positron candidates, summarized below, are designed to reject the energy deposits from photons or quark or gluon jets.

- $E_T > 25$ GeV for central electron and $E_T > 20$ GeV for plug electron,
- $E_{Iso} < 4$, where E_{Iso} is additional energy in an “isolation” cone with angular radius $R = \sqrt{(\Delta\phi)^2 + (\Delta\eta)^2} = 0.4$ centered on the electron,
- A small amount of hadronic energy relative to the EM energy,
- Cuts on the shower shape in the EM calorimeter and shower maximum detector,
- A track consistent with the position and energy measured in the calorimeter

COT tracks, reconstructed independently of the calorimeter measurement, can be compared to it in position and momentum. However, the coverage of the COT is limited to $|\eta_e| < 1.6$. To extend the measurement to higher $|\eta_e| < 2.8$, silicon stand-alone tracks are reconstructed. The plug electrons are required to have a good quality track to identify the charge of the electron.

Candidate $W \rightarrow e\nu$ events are required to have exactly one such e^\pm candidate as well as $\cancel{E}_T > 25$ GeV. We found 537,858 events in central and 176,941 events in plug with this requirements. The E_T distribution of electrons and the \cancel{E}_T used to reconstruct W events from $W \rightarrow e\nu$ decays are shown in Figure 4.

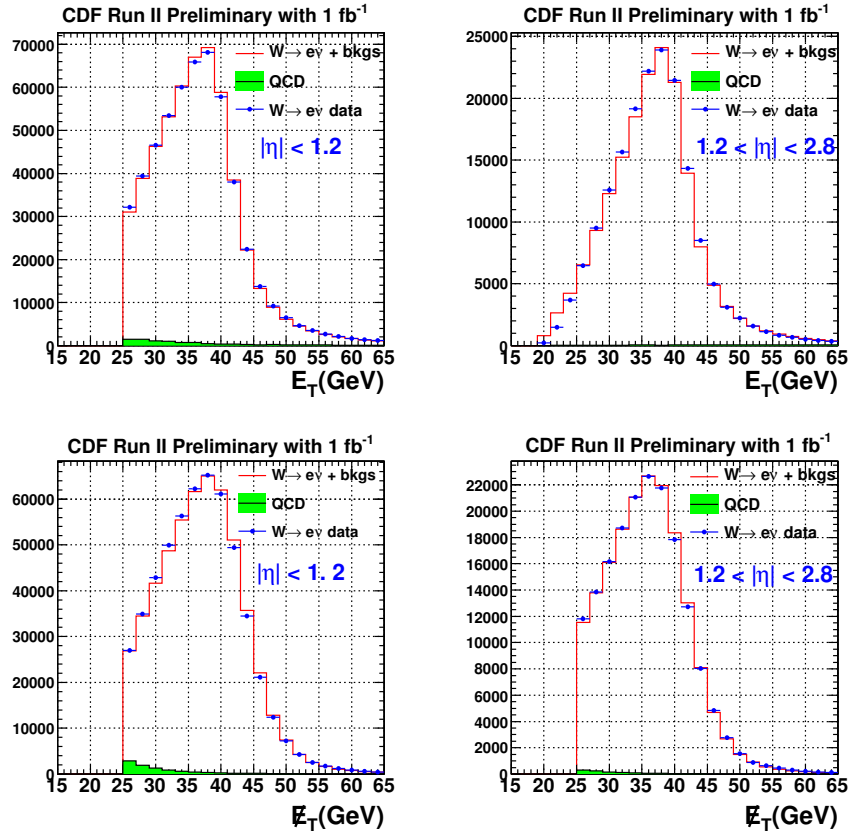


FIG. 4: The electron transverse energy (top) and missing transverse energy (bottom) in $W \rightarrow e\nu$ sample for the central electron(left) and the forward electron(right).

III. CORRECTIONS

In order to reconstruct the W charge asymmetry, the method described above needs to be corrected to account for several effects. These include:

- MC electron energy scale and resolution tuning
- correction to the \cancel{E}_T in events where the transverse mass of the electron and the \cancel{E}_T exceeds M_W
- correction for charge mis-identification in the central and plug tracking
- correction for the background
- correction for the effects of smearing and detector acceptance

We provide further detail below on the charge mis-identification, background and acceptance corrections.

A. Charge Mis-Identification

Good charge identification is crucial for the asymmetry measurement because the charge determines the sign of the weight factor, wt^\pm (see Eqn. 7), which corresponds to the number of W^\pm rapidity events. Therefore, charge misidentification of electrons changes the W charge asymmetry and the charge misidentification rate needs to be properly determined. We measure the charge fake rate using $Z \rightarrow ee$ events and the charge fake rate is defined as

$$f_{mis}(\eta) = \frac{N_{wrong-sign}(\eta)}{N_{right-sign}(\eta) + N_{wrong-sign}(\eta)}, \quad (8)$$

where $N_{wrong-sign}$ is the number of Z candidates where two electrons have the same sign, and $N_{right-sign}$ is the number where they have the opposite sign.

First, we need to identify a clean sample of $Z \rightarrow e^+e^-$ decays that we can use to study this charge misidentification. The ee invariant mass is required to be between 76 and 106 GeV/c^2 for Z s with two central electrons (central-central) and between 81 and 101 GeV/c^2 for Z s with one central and one plug electron (central-plug). We measure the charge fake rate from the selected Z candidates vs. η and we find the charge fake rate is highly dependent on η , as shown in Figure 5.

In order to have a charge mis-identification correction for our asymmetry, we need to describe the charge fake rate as a function of W rapidity. Thus, we derive a correction of charge fake rate such that it can be put into the acceptance correction from the charge fake rate vs. η in Figure 5. We express the total reconstructed number of positively and negatively charged events in Eqn. 9 and the total number of true charged events in Eqn. 10, below.

$$\begin{aligned} N_{obs}^+(wt^+) &= N_+^+(wt^+) + N_+^-(wt^+) \\ N_{obs}^-(wt^-) &= N_-^-(wt^-) + N_-^+(wt^-) \end{aligned} \quad (9)$$

$$\begin{aligned} N_{true}^+ &= N_+^+(wt^+) + N_-^+(wt^+) \\ N_{true}^- &= N_-^-(wt^-) + N_+^-(wt^-) \end{aligned} \quad (10)$$

$N_-^+(wt^+)$ is the number of truly positive charge events reconstructed with a negative charge and is a function of the weight factor (wt) in that bin of W rapidity. We then describe the number of true charged events with the reconstructed information and new factors in Eqn. 12 and 13, below.

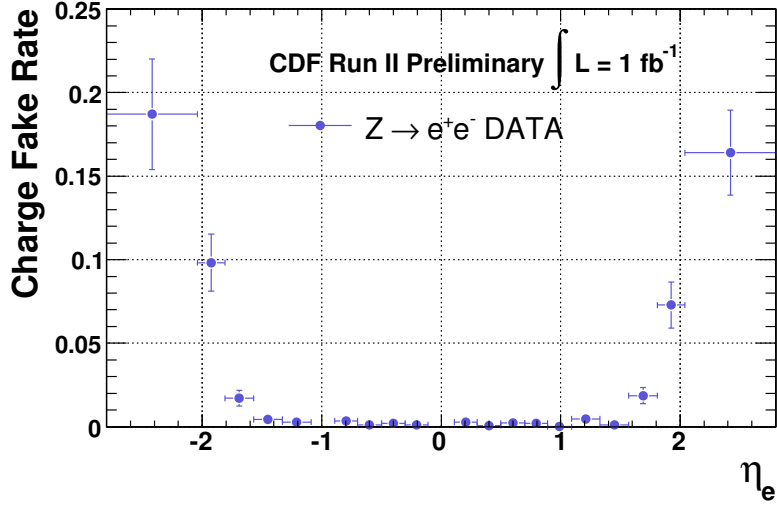


FIG. 5: The charge fake rate as a function of electron η .

$$\begin{aligned}
 N_{true}^+ &= [N_+^+(wt^+) + N_+^-(wt^+)] \times \frac{N_+^+(wt^+)}{[N_+^+(wt^+) + N_+^-(wt^+)]} \\
 &\quad + [N_-^-(wt^+) + N_-^+(wt^+)] \times \frac{N_-^-(wt^+)}{[N_-^-(wt^+) + N_-^+(wt^+)]} \\
 &= N_{obs}^+(wt^+) \times (1 - \rho^+(wt^+)) + N_{obs}^-(wt^+) \times (\rho^-(wt^+))
 \end{aligned} \tag{11}$$

$$\begin{aligned}
 N_{true}^- &= [N_-^-(wt^-) + N_-^+(wt^-)] \times \frac{N_-^-(wt^-)}{[N_-^-(wt^-) + N_-^+(wt^-)]} \\
 &\quad + [N_+^+(wt^-) + N_+^-(wt^-)] \times \frac{N_+^-(wt^-)}{[N_+^+(wt^-) + N_+^-(wt^-)]} \\
 &= N_{obs}^-(wt^-) \times (1 - \rho^-(wt^-)) + N_{obs}^+(wt^-) \times (\rho^+(wt^-))
 \end{aligned} \tag{12}$$

Therefore, we define the four charge fake rates in Eqn. 13, below, that are $\rho^+(wt^+)$, $\rho^+(wt^-)$, $\rho^-(wt^-)$ and $\rho^-(wt^+)$, as the reconstructed charge and the weight factors of the two W rapidity solutions. However, since this correction depends on the W rapidity, it must be iterated for the measurement.

Since we know the electron pseudo-rapidity and the charge fake rate corresponding to the pseudo-rapidity per event, we can represent the four charge fake corrections with the measured charge fake rate in the η bin as shown in Figure 5.

$$\begin{aligned}
\rho^+(wt^+) &= \frac{N_+^-(wt^+)}{N_+^+(wt^+) + N_+^-(wt^+)} \\
\rho^+(wt^-) &= \frac{N_+^-(wt^-)}{N_+^+(wt^-) + N_+^-(wt^-)} \\
\rho^-(wt^-) &= \frac{N_-^+(wt^-)}{N_-^-(wt^-) + N_-^+(wt^-)} \\
\rho^-(wt^+) &= \frac{N_-^+(wt^+)}{N_-^-(wt^+) + N_-^+(wt^+)}
\end{aligned} \tag{13}$$

B. Background correction

We take into account three backgrounds: $Z \rightarrow e^+e^-$, $Z \rightarrow \tau^+\tau^-$ and QCD. Note that we consider the $W \rightarrow \tau\nu \rightarrow e\nu$ as signal and it is included in the signal acceptance. For the $Z \rightarrow e^+e^-$ and $Z \rightarrow \tau^+\tau^-$ background estimate, we rely on MC. However, for the QCD background estimate we use a technique for estimating the QCD background by fitting the isolation distribution of the electrons [5]. We fit the data to a signal template from $Z \rightarrow e^+e^-$ data and a background template from dijet events in data. We also perform the fit separately for $25 \text{ GeV} < \cancel{E}_T < 35 \text{ GeV}$ and $35 \text{ GeV} < \cancel{E}_T < 200 \text{ GeV}$. The fit results for central and forward electrons are shown in Figure 6. In Figure 7 we show the QCD background rapidity distribution as a function of y_W . The background fractions and the fraction of $W \rightarrow \tau\nu$ we measure are summarized in Table I.

| samples | central | | plug | |
|------------------------------|----------|--------------------------------------------|---------|--------------------------------------------|
| | events | fraction (%) | events | fraction (%) |
| DATA | 537858 | | 176941 | |
| $Z \rightarrow e^+e^-$ | 3173.36 | 0.59 ± 0.02 (stat.) | 955.48 | 0.54 ± 0.03 (stat.) |
| $Z \rightarrow \tau^+\tau^-$ | 487.21 | 0.09 ± 0.00 (stat.) | 179.81 | 0.10 ± 0.01 (stat.) |
| QCD | 6508.08 | 1.21 ± 0.14 (stat.) ± 0.15 (syst.) | 1185.50 | 0.67 ± 0.12 (stat.) ± 0.14 (syst.) |
| $W \rightarrow \tau\nu$ | 12370.73 | 2.30 ± 0.04 (stat.) | 3609.60 | 2.04 ± 0.05 (stat.) |

TABLE I: The predicted background contribution in $W \rightarrow e\nu$ candidates. The error represents the statistical uncertainty and the systematic uncertainty caused by our isolation fit method (QCD). Note that $W \rightarrow \tau\nu \rightarrow e\nu$ is not considered to be a background but is included in the signal acceptance for the W charge asymmetry analysis, and its contribution is shown in the last row.

C. Acceptance

The raw W charge asymmetry we measure must be corrected for detector acceptance and smearing effects to obtain the physical W asymmetry, which can be compared to theoretical calculations. We define a correction for the acceptance of kinematic cuts as a function of reconstructed y_W :

$$a^\pm(y_W) = \frac{\# \text{ of events from MC and simulation which pass cuts}}{\# \text{ of events from MC without cuts at generation level}}, \tag{14}$$

where the sign, \pm , indicates the charge of W boson. The acceptance depends on the charge of the W boson, and such effects need to be carefully studied and evaluated before being applied blindly in this analysis because of their direct impact on the charge asymmetry. We also apply corrections to the acceptance to account for the trigger efficiency (which is not simulated) measured from the data,

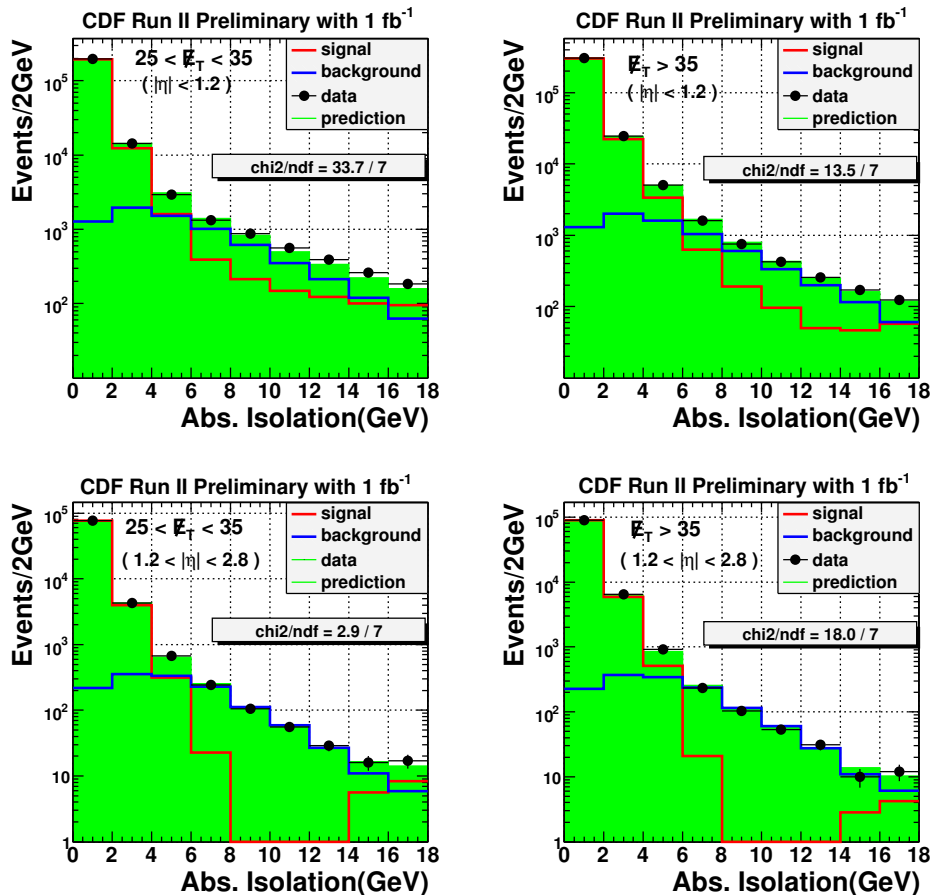


FIG. 6: Isolation fit distributions for the $W \rightarrow e\nu$ data (black dots), signal template (red), background template (blue) and the prediction from the fit (green). The results for two different \cancel{E}_T regions are presented : $25\text{GeV} < \cancel{E}_T < 35\text{GeV}$ (left) and $\cancel{E}_T > 35\text{GeV}$ (right), for central electrons (top) and for forward electrons (bottom).

the electron ID efficiency scale factors (data/MC, i.e., correcting the MC to match the data) and the charge fake rate also measured in the data. The acceptance correction is shown in Figure 8.

IV. SYSTEMATIC UNCERTAINTIES

We consider potentially significant sources of systematic uncertainty on the W charge asymmetry measurement. The uncertainties on the weighting factor given in Eqn 7 arise from uncertainties on the momentum distribution of quarks and gluons in the proton modeled with the PDF sets used. The choice of PDF set has an effect on the shape of the $d\sigma^\pm/dy_W$ distributions as well as the ratio of quark and anti-quark in the angular decay distribution.

We use the CTEQ6 error PDF sets [6] and perform the $d\sigma^\pm/dy_W$ production cross section and the angular distribution of $(1 \pm \cos\theta^*)^2$ for each error PDF set. We determine the uncertainty on the W charge asymmetry by checking how much the asymmetry values based on each calculation deviate from the value obtained using the best-fit PDF set.

We also studied the input PDFs for the valence quark, sea quark and gluon distributions affect our

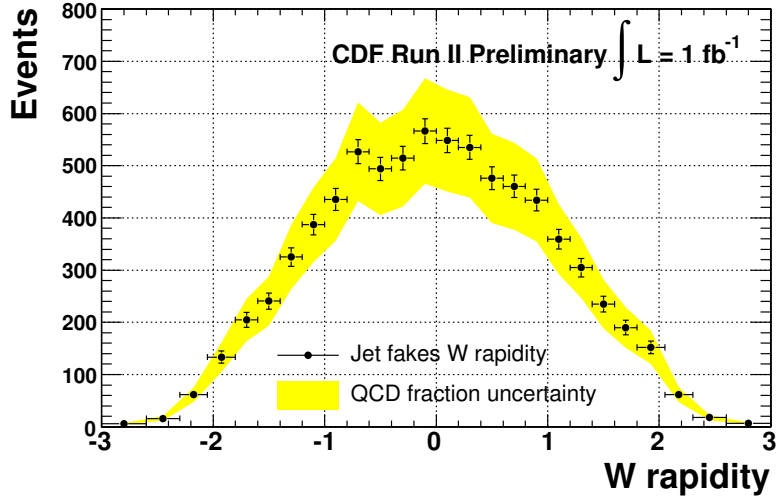


FIG. 7: QCD background rapidity distribution.

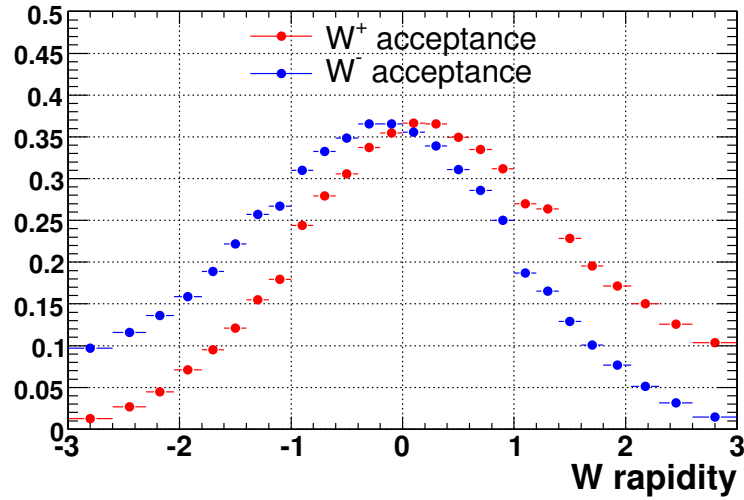


FIG. 8: The acceptance correction.

W charge asymmetry measurement and find it to be small. More details are found in the Appendix VI.

We also consider experimental sources of systematic uncertainty. The cluster E_T scale and resolution for electromagnetic sections of the calorimeter can change W rapidity and the asymmetry measurement. The asymmetry uncertainties are estimated as the changes in measured asymmetry for each candidate sample that occur when the cluster E_T is changed between its default and $\pm\sigma$ value. To account for the effect of the missing E_T scale in our $W \rightarrow e\nu$ sample, we consider the boson recoil energy (affected by multiple interactions) since an accurate model of the event recoil energy in the simulation is important for estimating the acceptance of the event \cancel{E}_T . The charge misidentification and backgrounds are crucial for the charge asymmetry measurement since both contributions can

| $ y_W $ | $\Delta A(y_W) (\times 10^{-2})$ | | | | | | | Stat. (1fb ⁻¹) |
|------------|------------------------------------|------------------|--------------|--------------|------------------|--------|------|----------------------------|
| | Charge Mis-ID | Bkg & Resolution | Energy Scale | Recoil Model | Electron Trigger | PDF ID | | |
| 0.0 - 0.2 | 0.02 | 0.04 | 0.01 | 0.11 | 0.029 | 0.02 | 0.03 | 0.31 |
| 0.2 - 0.4 | 0.01 | 0.09 | 0.04 | 0.22 | 0.08 | 0.07 | 0.08 | 0.32 |
| 0.4 - 0.6 | 0.02 | 0.11 | 0.06 | 0.22 | 0.13 | 0.17 | 0.15 | 0.33 |
| 0.6 - 0.8 | 0.03 | 0.15 | 0.07 | 0.34 | 0.14 | 0.30 | 0.22 | 0.32 |
| 0.8 - 1.0 | 0.03 | 0.20 | 0.07 | 0.42 | 0.11 | 0.47 | 0.24 | 0.34 |
| 1.0 - 1.2 | 0.04 | 0.18 | 0.08 | 0.33 | 0.09 | 0.69 | 0.27 | 0.38 |
| 1.2 - 1.4 | 0.05 | 0.18 | 0.15 | 0.67 | 0.06 | 0.78 | 0.28 | 0.43 |
| 1.4 - 1.6 | 0.04 | 0.14 | 0.14 | 1.10 | 0.04 | 0.85 | 0.28 | 0.50 |
| 1.6 - 1.8 | 0.08 | 0.12 | 0.26 | 0.92 | 0.03 | 0.89 | 0.29 | 0.55 |
| 1.8 - 2.05 | 0.22 | 0.13 | 0.31 | 0.82 | 0.06 | 0.80 | 0.34 | 0.62 |
| 2.05 - 2.3 | 0.44 | 0.21 | 0.53 | 0.59 | 0.17 | 0.85 | 0.42 | 0.83 |
| 2.3 - 2.6 | 0.45 | 0.19 | 0.62 | 0.40 | 0.27 | 0.86 | 0.50 | 1.10 |
| 2.6 - 3.0 | 0.14 | 0.10 | 0.60 | 0.43 | 0.28 | 0.65 | 0.53 | 2.30 |

TABLE II: Systematic uncertainties for the W production charge asymmetry. The values shows the correlated uncertainties for both positive and negative rapidities.

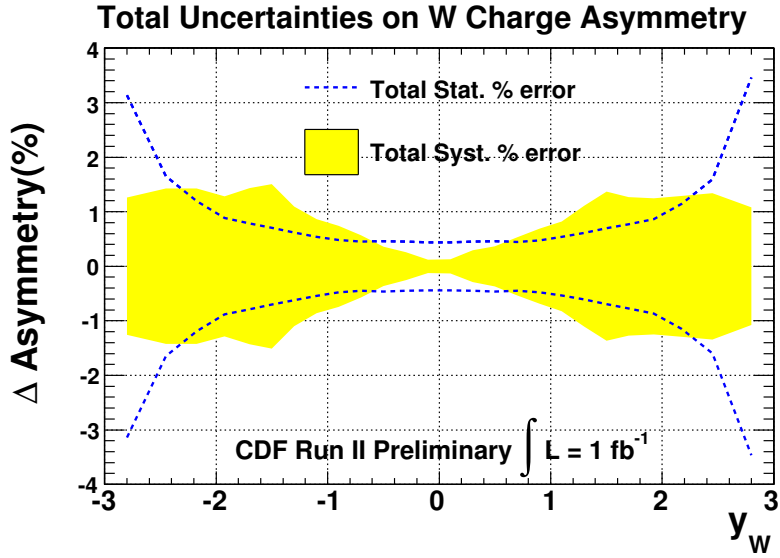


FIG. 9: Total systematic uncertainty for the W production charge asymmetry measured in % (yellow band) compared to the statistical uncertainty (blue dashed line).

directly change our result.

In Table II, we summarize the systematic uncertainties of the the W boson charge asymmetry measurement and can be compares with the statistical uncertainty obtained in this 1 fb⁻¹ measurement. Figure 9 shows the total systematic uncertainty on the asymmetry (fractional uncertainty measured in %) compared to the statistical uncertainty. The effect of the dominant systematic uncertainties due to uncertainties in electron ID efficiencies (ID), the charge mis-identification rate (CFR), the ratio of anti-quarks and quarks in the proton due to uncertainties in PDFs, and the recoil energy scale are shown in Figure 10.

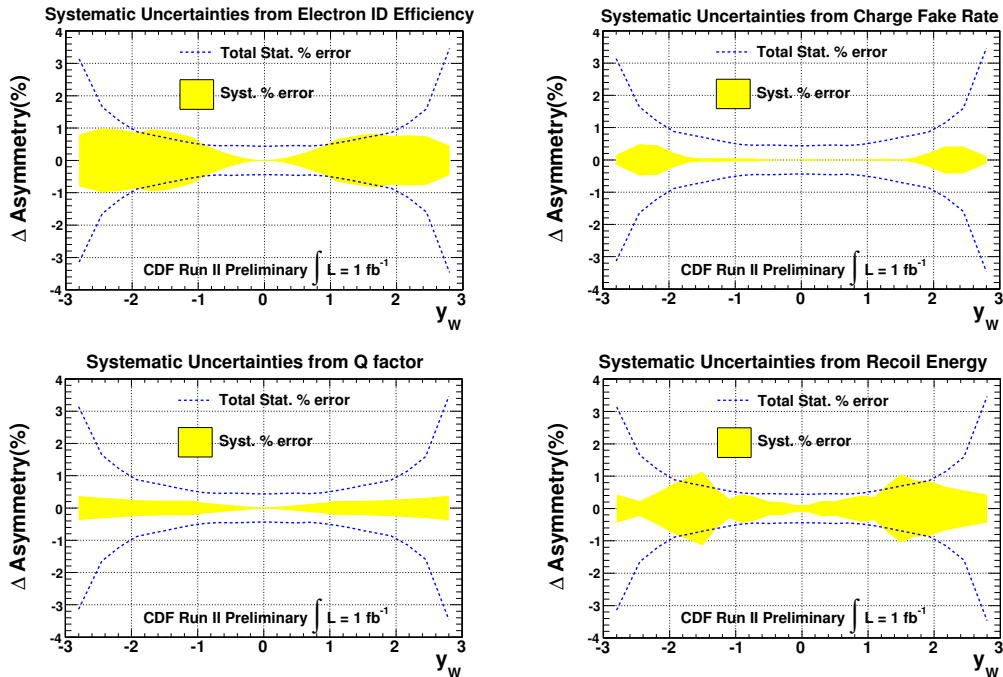


FIG. 10: The effects of electron E_T scale uncertainty (a), energy resolution uncertainty (b) and the recoil energy scale uncertainty (c) on the W charge asymmetry.

| $ y_W $ | $\langle yW \rangle_{m_W}$ | $A(y_W)$ | σ_{sys} | $\sigma_{sys+stat}$ |
|------------|------------------------------|----------|----------------|---------------------|
| 0.0 - 0.2 | 0.10 | 0.020 | ± 0.001 | ± 0.003 |
| 0.2 - 0.4 | 0.30 | 0.057 | ± 0.003 | ± 0.004 |
| 0.4 - 0.6 | 0.50 | 0.081 | ± 0.004 | ± 0.005 |
| 0.6 - 0.8 | 0.70 | 0.117 | ± 0.006 | ± 0.006 |
| 0.8 - 1.0 | 0.89 | 0.146 | ± 0.007 | ± 0.008 |
| 1.0 - 1.2 | 1.09 | 0.204 | ± 0.008 | ± 0.010 |
| 1.2 - 1.4 | 1.29 | 0.235 | ± 0.011 | ± 0.012 |
| 1.4 - 1.6 | 1.49 | 0.261 | ± 0.014 | ± 0.015 |
| 1.6 - 1.8 | 1.69 | 0.303 | ± 0.014 | ± 0.014 |
| 1.8 - 2.05 | 1.91 | 0.355 | ± 0.013 | ± 0.014 |
| 2.05 - 2.3 | 2.15 | 0.436 | ± 0.013 | ± 0.016 |
| 2.3 - 2.6 | 2.40 | 0.537 | ± 0.014 | ± 0.018 |
| 2.6 - 3.0 | 2.63 | 0.642 | ± 0.012 | ± 0.026 |

TABLE III: The W production charge asymmetry with total systematic and statistical uncertainties.

V. RESULTS

We present a direct measurement of the W production charge asymmetry using an integrated luminosity of 1 fb^{-1} . We use a new analysis method which directly reconstructs the W rapidity. We consider two possible W rapidity solutions because of the unknown longitudinal momentum of the neutrino from the W decay. We determine the relative contribution of the event to the two solutions according to the $V - A$ decay structure of the weak interaction and the dependence of W boson rapidity upon the differential cross-section, $d(\sigma_W)/dy$.

The W boson charge asymmetry for each $|y_W|$ bin with the total systematic uncertainty and the

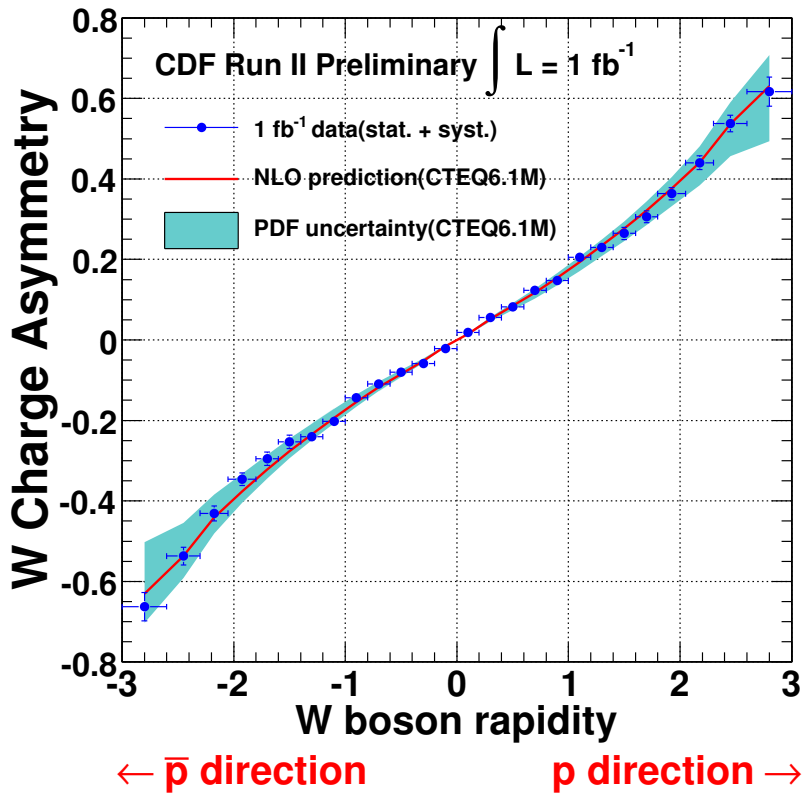


FIG. 11: The corrected W production charge asymmetry. The blue points represent the data and the error bars indicate the total uncertainty (stat.+ syst.). The red curve represents the NLO prediction using CTEQ6.1M PDFs and the blue band represents the PDF uncertainty from the corresponding PDF errors.

statistical uncertainty obtained in this 1 fb^{-1} measurement is summarized in Table III where the average $\langle |y_W| \rangle_{m_W}$ indicates an average value of W^+ and W^- rapidity in each y_W bin and at a fixed W mass, $m_W = 80.403 \text{ GeV}/c^2$. In Figures 12 and 13 we show the measured asymmetry, $A(|y_W|)$, combining the positive and negative y_W bins. We compare both to an NLO prediction with CTEQ6.1M PDFs [6] and also to an NNLO prediction [7] using MRST2006 PDFs [8] and their corresponding error PDFs, and find good agreement.

VI. APPENDIX

The goal of this section is to test how the valence quark, sea quark and gluon distributions affect our W charge asymmetry measurement. To do this study a Monte Carlo sample is generated using the MC@NLO program [4] with NLO QCD calculation and CTEQ6.1M PDFs to determine the quark and gluon distributions involving the W boson production.

The momentum fraction, x , is directly related to the rapidity of the W boson, and so it might be expected that changes of PDFs in a limited x range will affect a narrow region of rapidity. However, input PDFs are used in many cases to distinguish between two solutions, and therefore, a change in the input PDFs in a particular x range can actually affect a broader ranges of rapidities than one might naively expect. Both types of effects can be seen in the studies below. The effects on our measurement

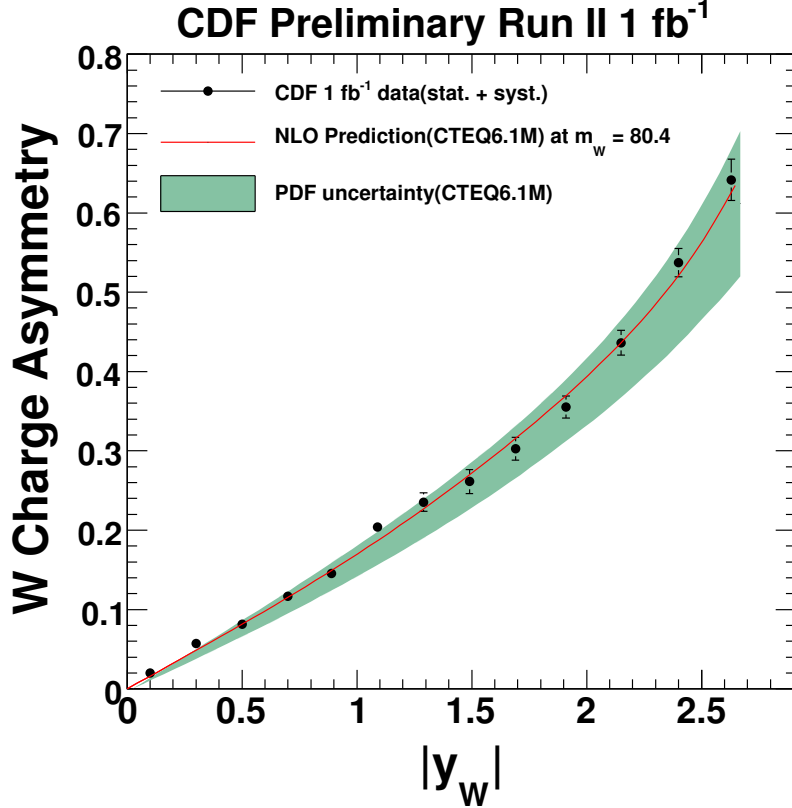


FIG. 12: The measured asymmetry, $A(|y_W|)$, compared to the NLO prediction with CTEQ6.1M PDFs.

are independently estimated for the valence quarks, sea quarks and the gluon distribution. The valence and sea quarks distribution are determined as $q_v(x) = q(x) - \bar{q}(x)$ and $q_s(x) = 2 \times \bar{q}(x)$ since the Monte Carlo sample has only quarks and anti-quarks distributions.

$$\begin{aligned}
 q_v(x) &= q_v(x) + 5\% \times q_v(x) \\
 q_s(x) &= q_s(x) + 5\% \times q_s(x) \\
 g(x) &= g(x) + 20\% \times g(x),
 \end{aligned}
 \tag{15}$$

where $g(x)$ is gluon distribution.

In the first study, the valence quark distributions within a fine x bin are increased by 5% (Eqn. 15), where the distributions for both proton and antiproton are changed while keeping the $d(x)/u(x)$ and $\bar{d}(x)/\bar{u}(x)$ constant. Then the rapidity of W boson is reconstructed again using our analysis method. The result of measured W charge asymmetry corresponding reweighted PDFs is compared with the initial asymmetry and the difference is examined. We show the x range for which we find the largest differences in the measured W charge asymmetry in Figure 14.

A similar study varying the weight of up and down sea quarks by +5% is shown in Figure 15, again for the x range with the largest difference. For the gluon distribution, the effect on our measurement is negligible for all x range, an example x range shown in Figure 16. Note that the effects of even these large changes in the quark and gluon distributions is small ($\lesssim 0.003$) compared with the statistical uncertainty ($\gtrsim 0.004$). This study allows one to estimate the effect on this W asymmetry measurement from the variation of input parton distribution functions.

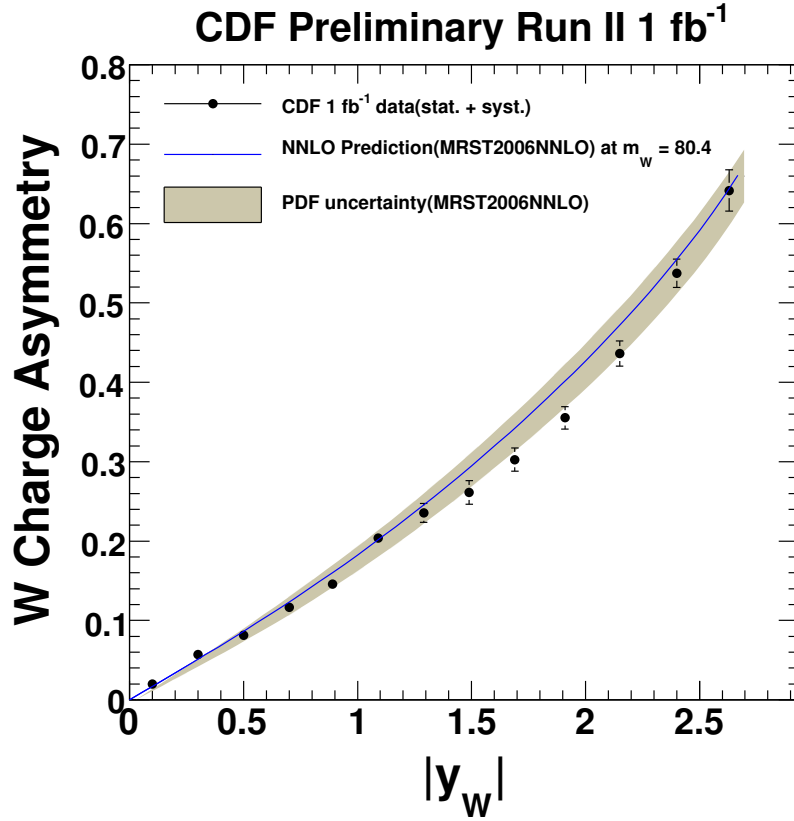


FIG. 13: The measured asymmetry, $A(|y_W|)$, compared to the NLO prediction with MRST2006 PDFs.

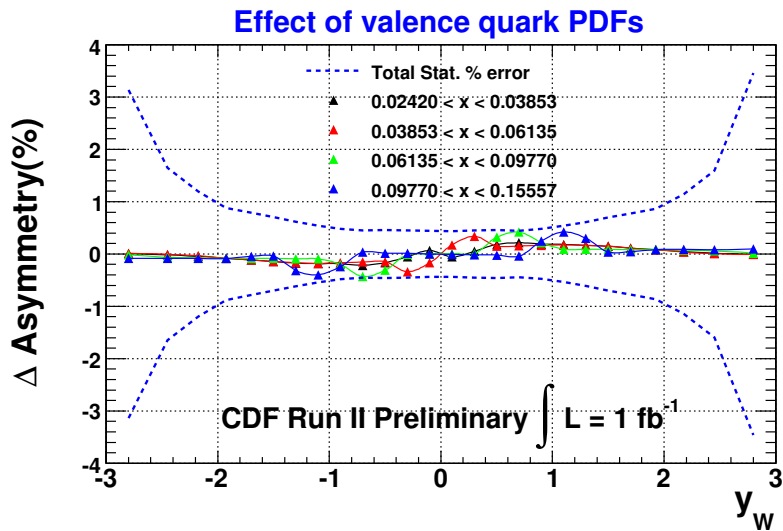


FIG. 14: The shift of the W charge asymmetry when the valence quark distribution is weighted by +5% in the high x region.

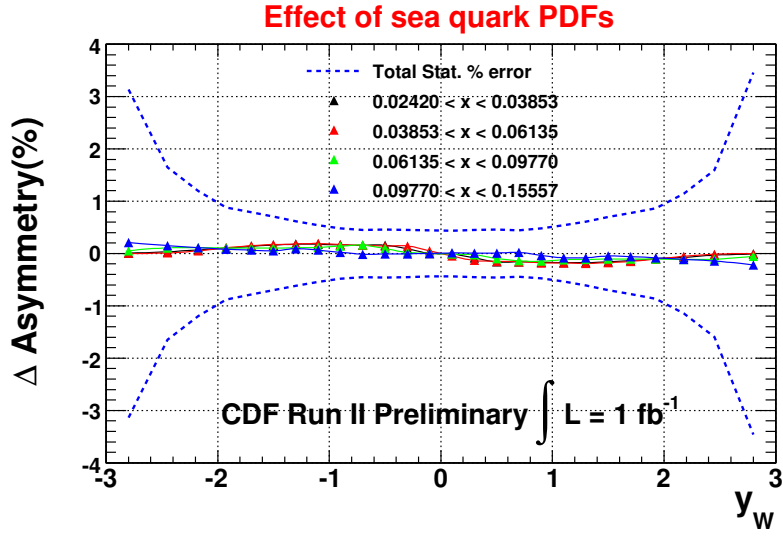


FIG. 15: The shift of the W charge asymmetry when the sea quark distribution is weighted by +5% in the high x region.

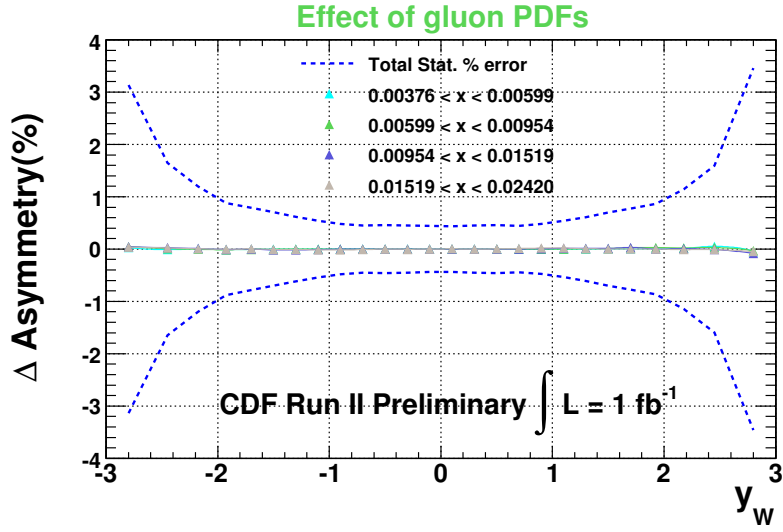


FIG. 16: The shift of the W charge asymmetry when the gluon distribution is weighted by +5% in the low x region.

-
- [1] A.D. Martin *et al.*, *Phys. Rev.* **D 50**(1994)6734.
 - [2] Qun Fan *et al.*, CDF Note 5566.
 - [3] D. Acosta *et al.*, *Phys. Rev.* **D 71**(2005)051104.
 - [4] S. Frixione, P. Nason and B.R. Webber, Matching NLO QCD and parton showers in heavy flavour production, *J. High Energy Phys.***0308** (2003) 007, hep-ph/0305252.

- [5] B-Y. Han *et al.*, "Backgrounds in $W \rightarrow e\nu$ for the W Production Charge Asymmetry Analysis", CDF note 8196.
- [6] J. Pumplin *et al.*, "New generation of parton distributions with uncertainties from global QCD analysis", hep-ph/0201195
- [7] C. Anastasiou *et al.*, Phys. Rev. **D69**, 094008 (2004)
- [8] A. D. Martin *et al.*, hep-ph/0706.0459; A. D. Martin *et al.*, Eur. Phys. J., **C28**, 455 (2003)